Handling performance of an 8x8 combat vehicle

IOP Conf. Series: Materials Science and Engineering **973** (2020) 012009 doi:10.1088/1757-899X/973/1/012009

Handling performance of an 8x8 combat vehicle

M Ahmed[1], M El-Gindy[1] and H Lang[1]
[1]Automotive, Mechanical and Manufacturing Engineering, Faculty of Engineering and Applied Science, 2000 Simcoe St. N, Oshawa, Ontario, Canada, L1H 7K4

Moataz.ahmed@uoit.net.

Abstract. In this research paper, the handling stability of an 8x8 combat vehicle will be assessed using two different control systems. The first technique utilizes a Torque Vectoring Controller (TVC) to control the vehicle yaw rate to meet the desired value. The second technique utilizes an Active Rear-axles Steering (ARS) to minimize the vehicle sideslip. TVC will be designed as a Single Input Single Output (SISO) control problem using a Sliding Mode Control (SMC) technique, while an Optimal Linear Quadratic Regulator (LQR) will be utilized to develop the ARS controller. The two controllers will be evaluated against a conventional vehicle with fixed rear axles. TruckSim software is used in corporation with Matlab/Simulink to implement and assess the controllers using Double Lane Change (DLC) over high and low coefficient of friction road surfaces at various speeds. The results give an insight into the driving conditions at which each controller is utilized and introduce a novel method to coordinate the integration between both controllers for integrated chassis applications.

1. Introduction

Ground vehicle handling stability had great attention during the last decades to stabilize the vehicle during a sudden maneuvers and cornering which can lead to rollover or loss of control. In general, improving the vehicle lateral stability is applied through two methods. The first is Direct Yaw Control (DYC) which can be designed by applying a corrective yaw moment to the vehicle to meet a desired signal. In addition, DYC can be implemented either by redistribute traction forces in case of Torque Vectoring Control (TVC) or braking forces in case of Differential Braking (DB)[1]. The second method to control the vehicle handling is Active Steering Control (ASC). This method aims to control the yaw motion by generating additional lateral forces at the front tires in case of Active Front Steering (AFS) [2]or at the rear tires in Active Rear Steering (ARS) as in [3]or by integrating both[4].

Despite of the effectiveness of the DYC and ASC systems, DYC systems are limited to the traction forces between the tires and the road surface, while the ASC systems are limited by the saturation of the generated lateral forces of the steered tires. Therefore, many researchers attempted to combine both controllers [5, 6]. This combination technique allows the vehicle to reach the maximum permissible stability.The combination of the controllers is known as Integrated Chassis Controller (ICC) which is developed using two approaches: top-down or bottom-up. In top-down approach all actuators are considered in one controller while in bottom-up method each controller is designed separately, and a low lever controller is used as a coordinator.

Several researches integrate ASC and DYC using top-down method such as in [7-9] where Linear Parametric Variables (LPV)-H_∞ was utilized. Also Predictive Controller (MPC) was used widely in the integration as in [10, 11]. Furthermore, optimization based control methods were introduced as in[12, 13]. Despite of the advantages of this method, it is not preferred in automotive research as adding or

modify individual controller is not supported and required redesigning the whole controller. In contrast, bottom-up approach support this without affecting other controllers. Therefore, this method is recently used in research as in [14-17] , which require a coordinator between the controllers and often gave a preference to a controller over another. However, the criteria for giving priority to one controller with respect to another was not considered in previous studies and need more justification. Besides, still there is no scheme to follow to add prospective controllers.

Multi-wheel vehicles offer several advantages as it has higher stability and fault tolerant capabilities than two-axle vehicles. Despite its enormous advantages, most of previous work only considered studying the stability of two axles vehicle and fewer showed concerns to study multi axles vehicle as in [18-20], which was the motivation of applying this study on an eight Wheel Drive (8WD)-four axles combat vehicle.

In this paper, the influence of ARS and TVC on lateral stability nd handling performance of a Multi-wheeled combat vehicle is investigated. Virtual testing of the controllers over low and high coefficient of friction surfaces at low and high speed is performed. In addition, the paper aims to give an insight into the advantages and disadvantages of each controller and define a performance map that can illustrate a region of priority of each controller. In addition, this performance map can be used as a novel and general scheme to integrate both controllers and future controller.

The paper is arranged as follows: At first, an ARS system is designed introducing a new configuration by utilizing the active and independent steering of the 3^{rd} and 4^{th} axles to minimize the vehicle sideslip. The control signal consists of two terms: feed forward and feedback terms. The feed forward term is designed based on the steady-state mathematical model of the vehicle and relates the steering of the 4^{th} and 3^{rd} axles to Akerman steering geometry. In addition, an LQR controller is developed to generate the feedback term, where the 3^{rd} and 4^{th} axles are steered independently. Second, TVC is developed using SMC to establish a corrective moment to control the vehicle yaw rate and match a reference yaw signal. After that, the controllers' performance is evaluated and compared with the uncontrolled vehicle using DLC maneuver and a performance map is introduced proposing a new integration technique. Finally, the conclusion comes at the end to summarize the paper and state the advantages and disadvantages of each controller.

2. Vehicle Bicycle Model

A two degrees of freedom bicycle vehicle model of the 4-axle combat vehicle is shown in figure 1. This model is used to derive the mathematical equations needed in the design of the active rear-axle steering (ARS) controller using LQR and the Zero Sideslip (ZSS) controller. Furthermore, the model is used to derive the reference model for the torque vectoring controller (TVC). The model is linearized and simplified by making the following assumptions:

- The model presents the vehicle in the yaw plane.
- Constant longitudinal velocity.
- Small slip and steering angles.
- Linear tire characteristics.

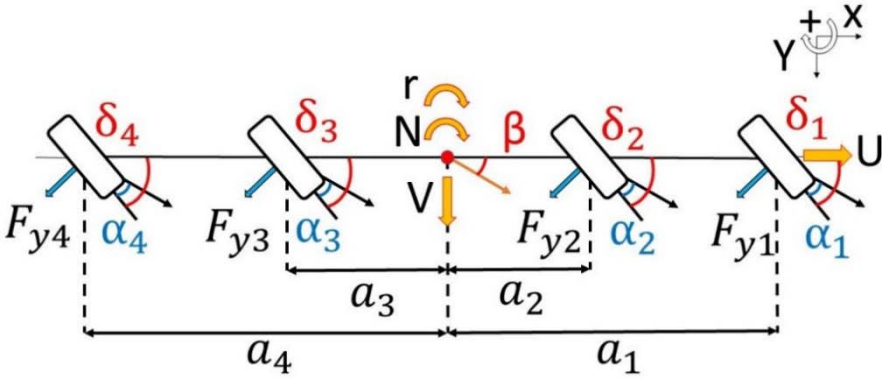

Figure 1.8x8 vehicle bicycle model.

The following equations present the vehicle mathematical model under the assumptions mentioned above, where M is the vehicle mass, U and V are the longitudinal and lateral velocities respectively, $\dot{V}$ lateral speed rate of change, r and $\dot{r}$are the vehicle yaw rate and yaw acceleration respectively, I_{zz} is the vehicle mass moment of inertia about the Z-axis,a_i is the distance from each axle i to the vehicle Center of Gravity (CG), where the axles ahead the vehicle CG have a positive sign, while the axles behind the CG takes a negative sign. N is an external yaw moment, F_{yi} is the cornering forces for each axle (combined right and left tire), $C_{\alpha i}$ is the combined cornering stiffness for each axleα_i the average slip angle, δ_i is the average steering angle, β is the vehicle sideslip, k_{21} is the ratio between the 1st and 2nd average steering angles, and k_{34} is the ratio between the 3rd and 4th average steering angles.

Lateral motion:

$$M\left(\dot{V} + Ur\right) = \sum_{i=1}^{4} F_{yi} \cos\delta_i \qquad (1)$$

Vehicle sideslip:

$$\beta = \frac{V}{U} \qquad (2)$$

Slip angles:

$$\alpha_i = \delta_i - tan^{-1}\left(\beta + \frac{a_i r}{U}\right) \qquad (3)$$

Lateral forces under linear tire characteristics:

$$F_{yi} = C_{\alpha i}\alpha_i \qquad (4)$$

Yaw motion:

$$I_{zz}\dot{r} = \sum_{i=1}^{4} a_i F_{yi} \cos\delta_i + N \qquad (5)$$

Substituting equations 2,3 and 4 into equation 1 and applying small angles approximation, the general vehicle yaw model in matrix form can be expressed in the state space form as:

$$\dot{x} = Ax + Bu + w \qquad (6)$$

$$y = Cx + Du \qquad (7)$$

where x and $\dot{x}$ are the states and the states rate of changes vectors, A is the states matrix, u and B are the input vector and the input matrix, respectively.C is the output matrix;D is the feedback matrix, which equals to zero, and w is the disturbance. Eventually, the state-space model of the system is:

$$\begin{bmatrix}\dot{\beta}\\ \dot{r}\end{bmatrix}=\begin{bmatrix}\frac{-\sum_{i=1}^{4}C_{\alpha i}}{MU} & \frac{-\sum_{i=1}^{4}a_iC_{\alpha i}}{MU^2}-1\\ \frac{-\sum_{i=1}^{4}a_iC_{\alpha i}}{I_{zz}} & \frac{-\sum_{i=1}^{4}{a_i}^2C_{\alpha i}}{I_{zz}U}\end{bmatrix}\begin{bmatrix}\beta\\ r\end{bmatrix}+\begin{bmatrix}\frac{C_{\alpha1}}{MU} & \frac{C_{\alpha2}}{MU} & \frac{C_{\alpha3}}{MU} & \frac{C_{\alpha4}}{MU} & \frac{0}{MU}\\ \frac{a_1C_{\alpha1}}{I_{zz}} & \frac{a_2C_{\alpha2}}{I_{zz}} & \frac{a_3C_{\alpha3}}{I_{zz}} & \frac{a_4C_{\alpha4}}{I_{zz}} & \frac{1}{I_{zz}}\end{bmatrix}\begin{bmatrix}\delta_1\\ \delta_2\\ \delta_3\\ \delta_4\\ N\end{bmatrix}+\begin{bmatrix}0\\ 0\end{bmatrix} \quad (8)$$

$$\begin{bmatrix}\beta\\ r\end{bmatrix}=\begin{bmatrix}1 & 0\\ 0 & 1\end{bmatrix}\begin{bmatrix}\beta\\ r\end{bmatrix}+\begin{bmatrix}0 & 00 & 0 & 0\\ 0 & 00 & 0 & 0\end{bmatrix}\begin{bmatrix}\delta_1\\ \delta_2\\ \delta_3\\ \delta_4\\ N\end{bmatrix} \quad (9)$$

3. Controllers Design

This section will be dedicated to designing ARS and TVC control systems. ARS will be designed based on optimal LQR methodology and a feed forward controller, so-called ZSS controller, while TVC will be designed based on SMC. The reference of each controller will be mentioned in the design procedure as apart from it.

3.1. Active rear steering control system (ARS)

As mentioned in the literature, ARS control has the benefits of generating excessive lateral forces without the increase of the vehicle sideslip which gives better tracking performance for the designed trajectory. Therefore, the reference and the main controller objective is to minimize vehicle sideslip.

3.1.1. LQR Control design. LQR is Multi input – Multi output (MIMO) controller based on solving a quadratic optimization problem under some constraints on the system states and the control inputs. The algorithm aims to solve the Riccati equation [21]as

$$A^TP+PA-PBR^{-1}B^TP+Q=0 \quad (10)$$

where$Q$ is the weight of the state, R is the input weight, and P is a positive definite matrix. As the control optimal control input u_{LQR} equal to the following:

$$u_{LQR}=-R^{-1}(B^TP)x \quad (11)$$

where x is the states.

Before applying the LQR on the general model, it should be manipulated to express the desired ARS model. By substituting the external yaw rate N by zero, separating the vehicle front steering angle as disturbance, and relating the average steering angle of the 2nd axles to the 1st one by the ratio k_{21}, where:

$$\delta_2=k_{21}\delta_1 \quad (12)$$

The ARS state-space model will be as follows:

$$\begin{bmatrix}\dot{\beta}\\ \dot{r}\end{bmatrix}=\begin{bmatrix}\frac{-\sum_{i=1}^{4}C_{\alpha i}}{MU} & \frac{-\sum_{i=1}^{4}a_iC_{\alpha i}}{MU^2}-1\\ \frac{-\sum_{i=1}^{4}a_iC_{\alpha i}}{I_{zz}} & \frac{-\sum_{i=1}^{4}{a_i}^2C_{\alpha i}}{I_{zz}U}\end{bmatrix}\begin{bmatrix}\beta\\ r\end{bmatrix}+\begin{bmatrix}\frac{C_{\alpha3}}{MU} & \frac{C_{\alpha4}}{MU}\\ \frac{a_3C_{\alpha3}}{I_{zz}} & \frac{a_4C_{\alpha4}}{I_{zz}}\end{bmatrix}\begin{bmatrix}\delta_3\\ \delta_4\end{bmatrix}+\delta_1\begin{bmatrix}\frac{C_{\alpha1}+k_{21}C_{\alpha2}}{MU}\\ \frac{a_1C_{\alpha1}+a_2k_{21}C_{\alpha2}}{I_{zz}}\end{bmatrix} \quad (13)$$

$$\begin{bmatrix}\beta\\ r\end{bmatrix}=\begin{bmatrix}1 & 0\\ 0 & 1\end{bmatrix}\begin{bmatrix}\beta\\ r\end{bmatrix}+\begin{bmatrix}0 & 0\\ 0 & 0\end{bmatrix}\begin{bmatrix}\delta_3\\ \delta_4\end{bmatrix} \quad (14)$$

The states and input weight matrices Q and R are tuned based on Bryson's rule [22-27], where

$$Q=\begin{bmatrix}\frac{1}{x_{1\,max.}^2} & 0\\ 0 & \frac{1}{x_{2\,max.}^2}\end{bmatrix}\text{ and }R=\rho\begin{bmatrix}\frac{1}{u_{1\,max.}^2} & 0\\ 0 & \frac{1}{u_{2\,max.}^2}\end{bmatrix} \quad (15)$$

where ρ is a tuning positive scaler, x_{1max} and x_{2max} are the maximum allowed error of the states (β and r), which can be determined as follow [28-30]:

$$\beta_{max} = tan^{-1}(0.02\mu g) \text{ and } r_{max} = \frac{0.75\,\mu g}{U} \quad (16)$$

And u_{1max} and u_{2max} are the average permissible steering angles for the 3rd and 4th axles, respectively.

3.1.2. ZSS controller. This controller is a feed forward controller. The control signal is determined by calculating the ratio between the 4th and 1st axle steering angles as a function of the vehicle speed ranging from 0 to 120 km/h, while the vehicle sideslip is set to be zero during steady-state motion (let $\dot{\beta} = \dot{r} = 0$). In addition, the ratio between the steering angles of the 4th and 3rdaxles, $k_{34,}$ is set based on Ackerman.

The steady-state equation of the vehicle can be written as follows:

$$\begin{bmatrix}\beta \\ r\end{bmatrix}_{ss} = -\begin{bmatrix} \frac{-\sum_{i=1}^{4} C_{\alpha i}}{MU} & \frac{-\sum_{i=1}^{4} a_i C_{\alpha i}}{MU^2} - 1 \\ \frac{-\sum_{i=1}^{4} a_i C_{\alpha i}}{I_{zz}} & \frac{-\sum_{i=1}^{4} a_i{}^2 C_{\alpha i}}{I_{zz}U} \end{bmatrix}^{-1} \begin{bmatrix} \frac{C_{\alpha 1}+k_{21}C_{\alpha 2}}{MU} & \frac{C_{\alpha 4}+k_{21}C_{\alpha 3}}{MU} \\ \frac{a_1 C_{\alpha 1}+a_2 k_{21} C_{\alpha 2}}{I_{zz}} & \frac{a_4 C_{\alpha 4}+a_3 k_{34} C_{\alpha 3}}{I_{zz}} \end{bmatrix} \begin{bmatrix}\delta_1 \\ \delta_4\end{bmatrix} \quad (17)$$

3.2. Torque vectoring control system

This section includes two subsections. The first section will discuss the SMC design and in the subsequent section, the reference model for the controller will be developed.

3.2.1. Sliding mode control (SMC) design. For the TVC system, a single input single output sliding mode controller is designed to ensure robust tracking performance to the reference yaw signal. As the objective of this controller is removing the error between the vehicle yaw rate and the reference one, the sliding surface is chosen as follows:

$$S = r - r_d \quad (18)$$

Substituting equation 5 in 18:

$$\dot{S} = e = \dot{r} - \dot{r_d} = \sum_{i=1}^{4} \frac{a_i F_{yi}}{I_{zz}} \cos\delta_i + \frac{N}{I_{zz}} - \dot{r_d} \quad (19)$$

To satisfy the reaching condition, the Lyapunov function is chosen as:

$$S\dot{S} \leq -K_{smc}|S| \text{where } K_{smc} > 0 \quad (20)$$

By using the law of constant reaching rate [31]:

$$\dot{S} = -K_{smc} sgn(s) \quad (21)$$

The chattering phenomena, which appears by using the previous discontinuous function can be lessened by using Quasi-Sliding mode utilizing the relay function as follows:

$$sgn(S) \approx \frac{S}{|S|+\varepsilon} \quad \text{Where } \varepsilon \text{ is very small and} > 0 \quad (22)$$

Finally, the controller, which is considered as the input corrective yaw moment to the vehicle *N* can be expressed as:

$$u_{SMC} = N = -\sum_{i=1}^{4} a_i F_{yi} \cos\delta_i + I_{zz}\dot{r_d} - I_{zz} K_{smc} \frac{S}{|S|+\varepsilon} \quad (23)$$

The control virtual stabilizing moment produced by the SMC is allocated using equation (24), where b is the vehicle trackwidth, and F_{xr}, F_{xl} are the summation of the driving forces on the right and left wheels respectively.

$$N = \frac{b}{2}(F_{xr} - F_{xl}) \qquad (24)$$

The driving forces have been optimized using quadratic cost function based on the constraints of the tire friction circle as in Mokhiamar et al. [32]with the additional assumption of negligible pitching motion due to vehicle acceleration and deceleration. However, the optimization procedure will not be mentioned as it is out of the scope of this paper. Furthermore, it is assumed that all the variables in the controller equations can be measured or determined. The determination of this date can be done by considering that the lateral forces of the tires can be determined by having the tire corner stiffness data as a function of the vehicle load and tire slip angle, and by assuming the ability to calculate the tire slip angle by measuring the vehicle sideslip and wheels steering angles by commercial available sensors.

3.2.2. SMC reference model. The steady-state model has been derived in Equation 18 and separating the steady-state yaw rate equation and substituting in δ_4 by zero as the rear two axles are fixed, the reference signal $r_d$is determined. However, the reference yaw rate signal has to be modified to match the vehicle response. This could be done by multiplying the signal by a Low Pass Filter (LPF) with a time constant τ such that:

$$r_{ref} = \frac{r_d}{\tau s+1} \qquad (25)$$

Noted that the reference yaw rate maximum value should be limited by the maximum desired yaw rate considered by [30] as in Equation 16.

4. Results and Discussion

The handling performance of each controller is evaluated and compared using modified Nato-DLC maneuver, where a curb is added in the beginning of the second lane to make the test more difficult. The test is performed at speed range from 30 to 80 km/h, where the surfaces COF is varied from 0.2 to 0.85. All cases will be been assessed in terms of trajectory stabilization time, yaw rate, lateral acceleration and velocity stability, and minimum lateral deviation from the designed trajectory.

A nonlinear 22 degrees of freedom 8x8 combat vehicle-model is used to evaluate the designed controllers, figure 2. The model was developed and validated in [33, 34] and used with TruckSim in previous researchers [20, 28]. Moreover, the simulation tests were performed using a TruckSim/Simulink environment and the controllers were implemented in Matlab/Simulink. Only, the results of the extreme cases at COF of 0.85 and 0.2 at vehicle speed of 80km/h will be introduced, while the results of all tests will be introduced at the end of this section.

Figure 2.8x8 vehicle configuration and the corresponding simulation model [35]

A DLC maneuver has been conducted on a dry surface (μ=0.85) at vehicle speed of 80 km/h. The simulation results are introduced in figure 3 and figure 4. Figure 3(a) shows the vehicle trajectory, which indicates that all cases completed the maneuver successively. However, the lateral deviation

from the desired path is illustrated at figure 3(b) where the minimum error is produced by the conventional vehicle followed by ARS, while TVC performs maximum error where the Rote Mean Square Error (RMSE) for all cases are 0.186, 0.216, and 0.259, respectively. The corresponding average front steering angle is indicated in figure 3(c). The minimum steering angle is produced by TVC, which gives the driver more controllability than other cases.

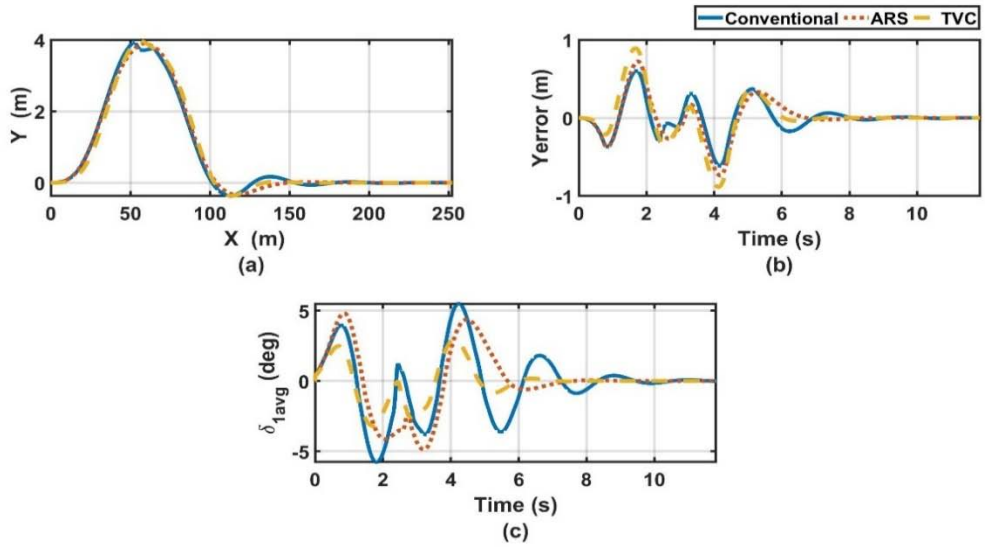

Figure 3. DLC maneuver at speed of 80km/h and μ= 0.85 a) Vehicle trajectory b) lateral error c) the corresponding average steering angle of the front axle.

Figure 4(a) shows the longitudinal velocity variation with time, where ARS produces the least variation, while TVC produces the most. The vehicle lateral acceleration and yaw rate response can be noticed in figure 4(b) and (c) respectively. The controlled vehicle is stabilized before the conventional one, where the TVC stabilizes the vehicle before the ARS by meantime 0.36 second. The vehicle side slip response is illustrated in figure 4(d), in which ARS produces the minimum vehicle slip andstabilize faster than TVC by 0.2 sec. Despite the preference of TVC in safety control systems on dry surfaces, it is recommended to utilize ARS in the case of autonomous applications due to its low lateral error, while it still gives an acceptable behavior in comparison with TVC.

Simulation results for repeating the test on a slippery surface with a coefficient of friction of 0.2 at speed of 80 km/h can be seen in figure 5 and figure 6. The vehicle trajectory is presented in figure 5(a), which shows that the conventional vehicle has been failed to complete the maneuver, while the controlled one did. However, TVC takes about 18.6 seconds to stabilize the vehicle trajectory, which is more than ARS by 9 seconds. Besides that, the RMSE for the lateral deviation from the desired trajectory in the case of ARS is 0.492, while in the case of TVC it reaches 2.037, which can be concluded from figure 5(b). figure 5(c) shows the corresponding average front steering angle, where ARS produces the minimum steering angle with maximum driver controllability. On the contrary, the conventional vehicle shows a saturation in the steering angle, which leads to loss of controllability and stability as well.

figure 6(a) shows the variation in the longitudinal velocity, where the least variation resulting from ARS. By observing the lateral acceleration and yaw rate response from figure 5(b) and (c), it can be noticed that TVC stabilizes the vehicle in about 20 seconds, which is almost double the time ARS takes to stabilize the vehicle. In figure 5(d), the vehicle side slip response with time indicates the same behavior as the yaw rate and lateral acceleration response. Furthermore, ARS produces the least side slip angle. It is concluded that the TVC behavior is dramatically deteriorating at very low COF, while

ARS shows higher reliability on slippery surfaces. Table 1and table 2summarize the vehicle response (settling time and lateral error) under each controller for DLC on a dry road and slippery road surfaces respectively.

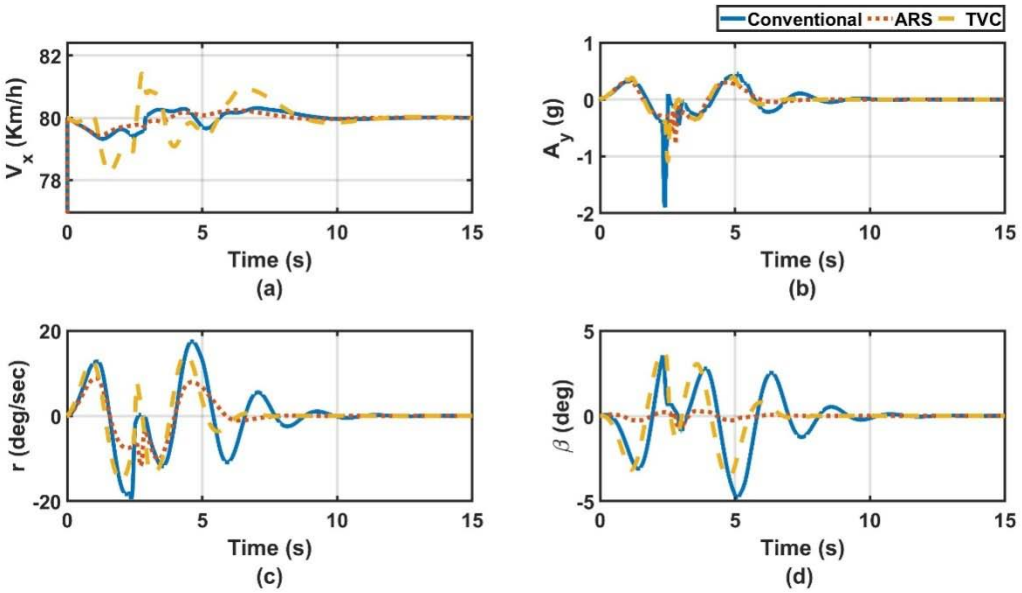

Figure 4. DLC maneuver at speed of 80km/h and μ = 0.85 a) vehicle longitudinal velocity b) lateral acceleration response c) yaw rate response d) vehicle sideslip.

Table 1. Lateral RMSE and Response for DLC at μ = 0.85 and speed of 80km/h.

Criteria	Conventional			ARS			TVC		
Lateral RMSE (m)	0.0542	0.0862	0.1862	0.0552	0.1065	0.2155	0.166	0.2015	0.259
Trajectory Settling time (sec.)	13.344	9.532	8.85	13.295	9.184	7.753	12.782	8.641	6.883
Lateral acceleration Settling time (sec.)	13.507	9.797	8.723	13.657	9.757	7.275	13.451	9.157	6.597
Yaw rate Settling time (sec.)	14.03	9.602	10.53	13.831	9.715	7.407	13.283	8.769	7.164
Side slip Settling time (sec.)	15.358	10.001	10.099	15.121	9.376	7.376	14.954	9.266	7.547

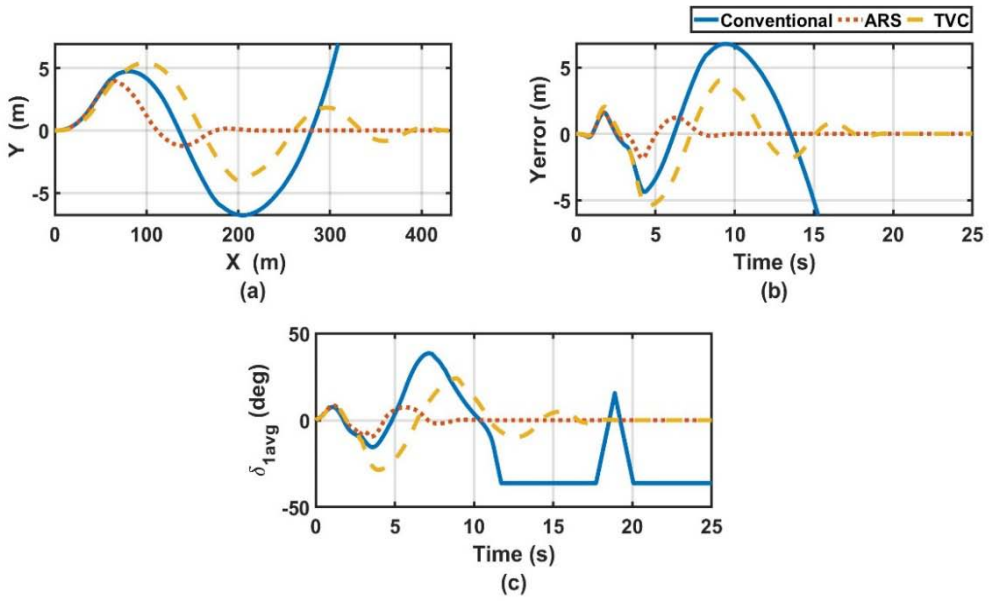

Figure 5. DLC maneuver at speed of 80km/h and μ = 0.2 a)Vehicle trajectory b) lateral error c) the corresponding average steering angle of the front axle.

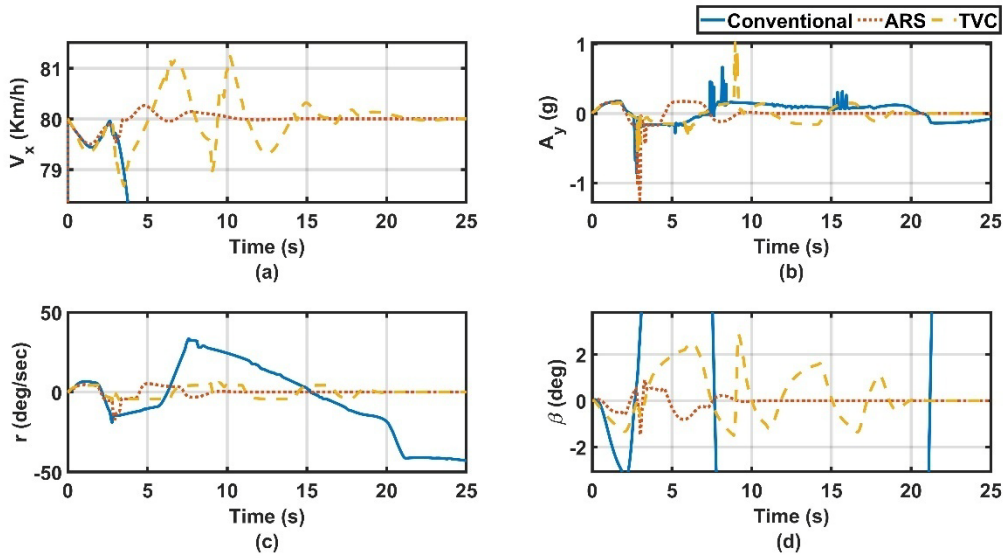

Figure 6. DLC maneuver at speed of 80km/h and μ = 0.2 a) vehicle longitudinal velocity b) lateral acceleration response c) yaw rate response d) vehicle sideslip

Table 2. Lateral RMSE and Response for DLC of μ = 0.2 and speed of 80km/h

Criteria	Conventional			ARS			TVC		
Lateral RMSE (m)	0.038	3.18		0.0452	0.284	0.494	0.1686	1.341	2.037
Trajectory Settling time (sec.)	14.10	19.81		13.134	11.003	9.474	13.679	17.401	18.635
Lateral acceleration Settling time (sec.)	13.97	18.99	Fail	13.512	10.541	8.956	14.078	18.229	19.545
Yaw rate Settling time (sec.)	14.14	19.82		13.63	10.579	10.108	13.699	18.858	20.262
Side slip Settling time (sec.)	15.16	19.78		15.098	10.032	9.829	14.953	19.294	20.37

To give a better insight into the advantages and preferences of each controller, the DLC maneuver is conducted at different surfaces with different COF at various speeds. The vehicle longitudinal velocity was varied from 30 to 80 km/h, while the COF changed from 0.2 to 0.85. The mean value of the time (settling time) for stabilizing the vehicle trajectory, lateral acceleration, yaw rate, and side slip is calculated. In figure 7(a) and (b), the inverse of the settling time, which denoted as Z-axis, plotted against the vehicle speed and road COF for ARS and TVC respectively, where the higher point on Z-axis indicates better stability and less settling time. It can be seen that at low COF and higher speed ARS gives much better performance than TVC, while at high COF and low-speed TVC is preferred over ARS. This preference decreases with the increase of speed at a high coefficient of friction road surface, where the difference is negligible.

Combining the two surfaces as in figure 8(a) and project the Line of Intersection (LOI) of the two surfaces on the X-Y plane (COF-Speed) can separate it into two areas in which one of the two controllers is favored. The difference between the settling time of each controller is calculated and merged with the LOI of the two controllers in figure 8(b). The driving condition that each controller has supremacy is illustrated, where TVC is preferred in the region above the LOI, while ARS is preferred below it. However, the difference between the settling time shows that there is a huge difference in behavior between the two controllers at low friction and high-speed region, which is decreased with the increase of the vehicle speed and the road COF and becomes less than 1 second above COF of 0.5. This figure clarifies that implementing ARS has the highest demand at extreme driving condition, at low COF and high speed. Moreover, if the small difference between both controllers is neglected, ARS could be implemented alone without the integration with TVC. Furthermore, if the two controllers are combined, figure 8(b) can be used for coordination with giving the percentage of contribution of each controller based on the settling time difference.

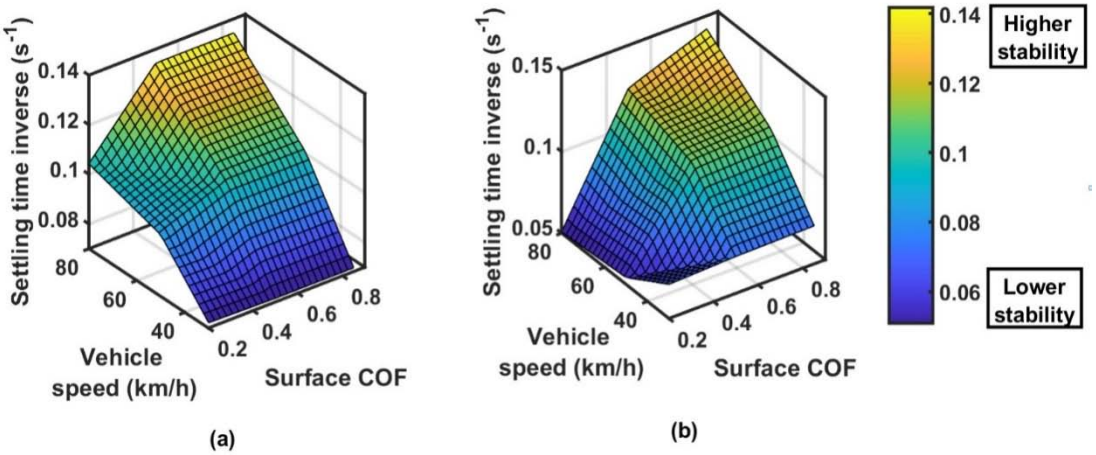

Figure 7. Controllers stability contour at various driving conditions a)ARS system b)TVC system.

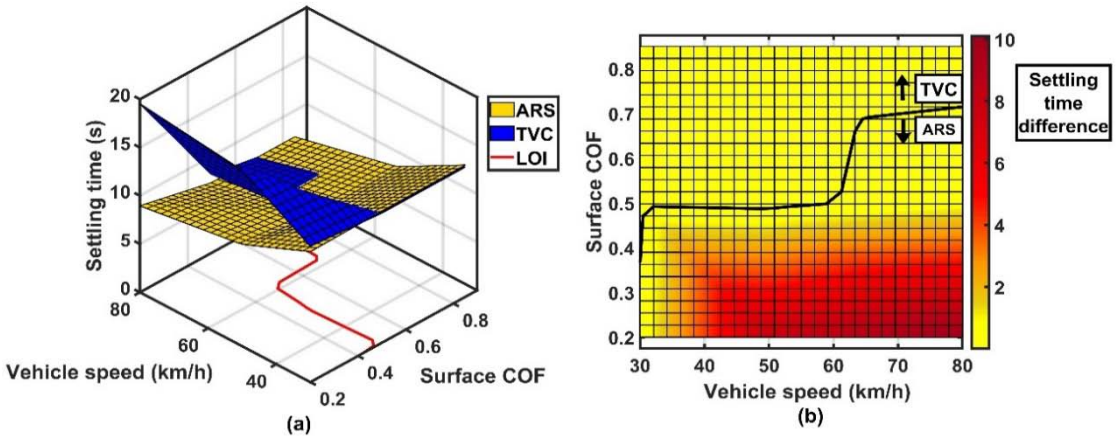

Figure 8.(a) Intersection of stability contours at various driving conditions (b) Region of preference.

5. Conclusions

In this paper, an 8x8 combat vehicle was used to implement and compare two chassis controllers. An ARS system has been developed using a combined feed forward controller and optimal Linear Quadratic Regulator (LQR) feedback controller and compared with Torque Vectoring Control (TVC) system which is designed using Sliding Mode Control (SMC) technique. Both controllers were separately evaluated and compared with conventional front steering vehicle. Double Lane Change (DLC)maneuver was used for evaluating and comparing the controllers at various vehicle speeds and road coefficient of friction. The results show that both controllers can enhance the handling performance and stability of the vehicle at all driving conditions. However, by comparing both controllers on a dry road surface, TVC offers more controllability and stability at high speed than ARS but with higher lateral error in comparison with the desired trajectory, which makes ARS recommended in the case of path follow maneuvers. On the contrary, ARS has notable superiority at extreme driving conditions such as driving on a very low coefficient of friction road surface and high speed, where there are low tire-ground traction forces. While the TVC is preferred at very low speeds. Moreover, the advantages and disadvantage of both controllers are summarized as follows:

- From the stabilization time perspective, TVC is slightly better than ARS while driving on a dry surface. In addition, TVC is recommended because of the higher degree of controllability it offers for the driver at high speed.
- ARS has superiority over TVC in case of driving on high slippery surfaces with high speed.
- ARS is also preferred due to the absence of the complications inthe reference model, which is essential for TVC, and the less need for parameter estimation and measurements than TVC.
- For path-following applications, ARS is recommended due to its lower lateral deviation from the desired trajectory.
- Economically, implementing the required component for TVC for all axles is relatively more expensive than implementing ARS for the rear axles only.

A novel method for coordinating both controllers is introduced for particular applications. This coordination is based on the road coefficient of friction, the vehicle speed, and the response time of each controller.

Finally, the integration of both controllers using the proposed coordination method can be a subject of future work. In addition, the differential braking should be examined in detail because of its simplicity and lower cost in comparison to the TVC.

References

[1] Asiabar AN and Kazemi R 2019 A direct yaw moment controller for a four in-wheel motor drive electric vehicle using adaptive sliding mode control.*P. I. Mech. Eng. K-J Mul.* p. 549-67.

[2] Ma X, et al. 2019 Cornering stability control for vehicles with active front steering system using TS fuzzy based sliding mode control strategy.*Mech. Syst. Signal Pr.***125**: p. 347-64.
[3] Park K, Joa E and Yi K 2019 Rear-Wheel Steering Control for Enhanced Maneuverability of Vehicles, SAE International.
[4] Zhao W, Qin X and Wang C 2018 Yaw and lateral stability control for four-wheel steer-by-wire system.*IEEE/ASME Trans. Mechatronics*. **23**(6): p. 2628-37.
[5] Yokoya Y, et al. 1990 Integrated control system between active control suspension and four wheel steering for the 1989 Celica, SAE Technical Paper.
[6] Kawakami H, et al. 1992 Development of integrated system between active control suspension, active 4WS, TRC and ABS, SAE Technical Paper.
[7] Selmanaj D, et al. 2013 Advantages of rear steer in LTI and LPV vehicle stability control. in *52nd IEEE Conference on Decision and Control*. IEEE. p. 3523-28.
[8] Wang R, Zhang H and Wang J 2013 Linear parameter-varying controller design for four-wheel independently actuated electric ground vehicles with active steering systems.*IEEE Trans. Control Syst. Technol.***22**(4): p. 1281-96.
[9] Jing H, et al. 2018 Robust H∞ dynamic output-feedback control for four-wheel independently actuated electric ground vehicles through integrated AFS/DYC.*Journal of the Franklin Institute*. **355**(18): p. 9321-50.
[10] Jalali M, et al. 2017 Model predictive control of vehicle stability using coordinated active steering and differential brakes.*Mechatronics*. **48**: p. 30-41.
[11] Mirzaeinejad H, Mirzaei M and Rafatnia S 2018 A novel technique for optimal integration of active steering and differential braking with estimation to improve vehicle directional stability.*ISA transactions*. **80**: p. 513-27.
[12] Nah J and Yim S 2019 Optimization of control allocation with ESC, AFS, ARS and TVD in integrated chassis control.*J. Mech. Sci. Technol.*: p. 1-8.
[13] Zhang J and Li J 2019 Integrated vehicle chassis control for active front steering and direct yaw moment control based on hierarchical structure.*T. I. Meas. Control*. **41**(9): p. 2428-40.
[14] Song J 2018 Integrated vehicle dynamic controls using active rear wheel steering and four wheel braking.*IJVSMT*. **13**(1): p. 26-43.
[15] Rahimi S and Naraghi M 2018 Design of an integrated control system to enhance vehicle roll and lateral dynamics.*T. I. Meas. Control*. **40**(5): p. 1435-46.
[16] Ahangarnejad AH, Melzi S and Ahmadian M 2019 Integrated Vehicle Dynamics System through Coordinating Active Aerodynamics Control, Active Rear Steering, Torque Vectoring and Hydraulically Interconnected Suspension.*Int. J. Auto. Tech-Kor*. **20**(5): p. 903-15.
[17] Termous H, et al. 2019 Coordinated control strategies for active steering, differential braking and active suspension for vehicle stability, handling and safety improvement.*Vehicle Syst. Dyn.***57**(10): p. 1494-529.
[18] Kim W, Yi K and Lee J 2011 Drive control algorithm for an independent 8 in-wheel motor drive vehicle.*J. Mech. Sci. Technol.***25**(6): p. 1573.
[19] Kim W, Yi K and Lee J 2012 An optimal traction, braking, and steering coordination strategy for stability and manoeuvrability of a six-wheel drive and six-wheel steer vehicle.*P. I. Mech. Eng. D-J Aut.***226**(1): p. 3-22.
[20] D'Urso P 2016 Development of H∞ control strategy for a multi-wheeled combat vehicle.
[21] Shinners SM 1998 *Modern control system theory and design*. John Wiley & Sons.
[22] Alves SBD 2012 Helicopter flight modeling and robust autonomous control with uncertain dynamics, Universidade da Beira Interior.
[23] Murray RM 2009 Optimization-based control.*California Institute of Technology, CA*. p. 111-28.
[24] Kalbat A 2013 Linear quadratic gaussian (lqg) control of wind turbines. in *2013 3rd International Conference on Electric Power and Energy Conversion Systems*. IEEE. p. 1-5.

[25] Manchester IR 2013 AMME4500: Guidance, Navigation, and Control Course Notes University of Sydney.
[26] Wang R, et al. 2016 Composite nonlinear feedback control for path following of four-wheel independently actuated autonomous ground vehicles.*IEEE Trans. Intell. Transp. Syst.***17**(7): p. 2063-74.
[27] Hespanha JP 2018 *Linear systems theory*. Princeton university press.
[28] Russell B 2018 Development and analysis of active rear axle steering for 8x8 combat vehicle.
[29] Odrigo A 2017 Development of multi-wheel drivetrain control system for future electric combat vehicle.
[30] Rajamani R 2011 *Vehicle dynamics and control*. Springer Science & Business Media.
[31] Liu J and Wang X 2012 *Advanced sliding mode control for mechanical systems*. Springer.
[32] Mokhiamar O and Abe M 2004 Simultaneous optimal distribution of lateral and longitudinal tire forces for the model following control.*J. Dyn. Sys., Meas., Control*. **126**(4): p. 753-63.
[33] Hillegass MJ, et al. 2004 Validating the directional performance of multi-wheeled combat vehicle computer simulation models. in *ASME 2004 International Mechanical Engineering Congress and Exposition*. American Society of Mechanical Engineers. p. 781-89.
[34] Hillegass MJ, et al. 2005 Validating the Vertical Dynamic Performance of a Multi-Wheeled Combat Vehicle Computer Simulation Model. in *ASME 2005 International Mechanical Engineering Congress and Exposition*. American Society of Mechanical Engineers. p. 31-40.
[35] Stryker November 2019 https://en.wikipedia.org/wiki/Stryker.